Full electron description of antiproton collisions with neon and argon atoms in the keV energy range

C. C. Jia [1,2] J. W. Gao [3] Y. Wu,[1] J. G. Wang,[1] and N. Sisourat [2,*]

[1]*Key Laboratory of Computational Physics, Institute of Applied Physics and Computational Mathematics, 100088 Beijing, China*

[2]*Sorbonne Université, Centre National de la Recherche Scientifique, Laboratoire de Chimie Physique-Matière et Rayonnement, 75005 Paris, France*

[3]*School of Physics, Hangzhou Normal University, 311121 Hangzhou, China*

(Received 4 September 2023; revised 16 January 2024; accepted 11 June 2024; published 2 July 2024)

We investigate keV collisions between antiprotons and the rare-gas atoms neon and argon. We use a correlated approach in which the eight electrons from the L shell of neon and M shell of argon are active and up to two-electron processes are included, going thus beyond the approximate theoretical approaches used so far. Our results show that the electronic correlation plays a major role in the single- and double-ionization processes. Furthermore, we show that two-electron processes contribute significantly to the electronic stopping power. These results apply to both target atoms studied in this paper and we therefore conclude that a correlated approach is in general necessary to obtain accurate antiproton electronic stopping-power cross sections. Our paper paves the way to a better understanding and knowledge of antiproton collision physics.

DOI: 10.1103/PhysRevA.110.012803

I. INTRODUCTION

Deceleration and transmission of antiprotons with keV-scale kinetic energies have recently attracted considerable attention (see, e.g., [1–3] and references therein) due to the development of the ELENA facility at CERN [4] and the associated experiments like the ALPHA, AEgIS, ASACUSA, BASE, and GBAR ones [5]. These experiments aim at testing fundamental symmetries to explain why antimatter is so scarce in our universe. Antiproton beams are also considered to treat cancer cells [6].

The energy-loss cross sections for a single collision between antiprotons and atoms and molecules are therefore relevant and important quantities. However, they are difficult to measure [3]. From a theoretical point of view, antiproton collisions with atomic and molecular hydrogen and helium have been widely investigated (see, e.g., [7,8] and references therein). Theoretical studies on larger collision systems are, however, scarce.

Antiproton collisions with neon and argon atoms represent the first step to go beyond the simple systems cited above. However, for neon the two most recent calculations disagree significantly. In both cases, the employed theoretical approach is only approximate: in [9], only single-electron transitions from the $2p$ shells are included. In [2], $2s$ and $2p$ shells are considered. Electronic correlation and many-electron processes are, however, only treated at a time-dependent density-functional theory level. To extend our understanding and knowledge of antiproton physics it is crucial to resolve these disagreements.

In this paper, we treat the collisions between antiprotons and neon and argon atoms using a correlated approach, going thus beyond the approximate theoretical approaches used so far. The eight electrons from the L shell of neon and M shell of argon are active and up to two-electron processes are included in our simulations. Moreover, we compare the results of this correlated method to those of an uncorrelated approach. Our results indicate that the electronic correlation electrons play a major role in computing accurately the single- and double-ionization cross sections. Furthermore, we show that two-electron processes contribute significantly to the stopping power. These results apply to neon and argon target atoms, therefore a correlated approach is in general necessary to obtain accurate antiproton stopping-power cross sections.

II. METHODS AND COMPUTATIONAL DETAILS

In the present paper, the cross sections of the electronic processes are calculated using a full-active-electron semiclassical asymptotic-states close-coupling approach which has been previously described in, e.g., [10–13]. Here we only outline the main features of the approach. The time-dependent Schrödinger equation is written as

$$\left[H - i\frac{\partial}{\partial t}\right]\Psi(\vec{\mathbf{r}}, \vec{R}(t)) = 0, \tag{1}$$

with electronic Hamiltonian

$$H = \sum_{i=1}^{N}\left[-\frac{1}{2}\nabla_i^2 + V_T(r_i) + V_P\left(r_i^p\right)\right] + \sum_{i=1}^{N}\sum_{j>i}^{N}\frac{1}{|\vec{r}_i - \vec{r}_j|}, \tag{2}$$

where $\vec{r}_i$, $\vec{r}_i^{\,p} = \vec{r}_i - \vec{R}(t)$ are the position vectors of the N electrons with respect to the center of mass of the target and projectile, respectively. The relative projectile-target position $\vec{R}(t)$ defines the trajectory, with $\vec{R}(t) = \vec{b} + \vec{v}t$ in the usual straight-line, constant velocity approximation: $\vec{b}$ and $\vec{v}$ are

*Contact author: nicolas.sisourat@sorbonne-universite.fr

the impact parameter and velocity, respectively. The term V_T (V_P) defines the electron-target (-projectile) nucleus potential. The Schrödinger equation [Eq. (1)] is solved by expanding the wave function onto a basis set composed of states of the isolated target partner as in [8], for a set of initial conditions (i.e., initial electronic state i, velocity v, impact parameter b). The probability of a transition $i \to f$ is given by the square of expansion coefficients c_f as

$$P_{fi}(v,b) = \lim_{t\to\infty} |c_f(t)|^2. \tag{3}$$

The corresponding cross sections can be calculated from these probabilities as follows:

$$\sigma_{fi}(v) = 2\pi \int dbbP_{fi}(v,b). \tag{4}$$

We use the aug-cc-pVDZ basis set [14], augmented with three Kaufmann functions [15] in order to describe the continuum. The eight electrons in the L shell of neon (M shell of argon) are active but only up to two electrons can be excited or ionized. About 17 900 configurations for neon (12 200 configurations for argon) are used to describe the pseudostates. Pseudostates with energy up to −122.1 a.u. for neon (−522.5 a.u. for argon) are kept in our calculations. These singly and doubly excited configuration interaction calculations are labeled CISD-2s2p for neon (CISD-3s3p for argon) hereafter. We checked the convergence of our results by comparison with that obtained with a larger basis set. Details of the two basis sets are given in Supplemental Material [16]. The difference between the SI cross sections obtained with the two basis sets employed in this paper is at most 10%. The DI cross sections, being smaller and in general more difficult to compute accurately, change by about 50% on average. Furthermore, to demonstrate the importance of the electronic correlation we compare the results of our correlated approach with an uncorrelated one for which only one electron can be excited or ionized (labeled CIS-2s2p for neon and CIS-3s3p for argon below). For the uncorrelated approach we use the same basis set as for the correlated one. Finally, we investigate the importance of the 2s shell in the case of antiproton-neon collisions by performing further calculations for which the corresponding electrons are frozen (labeled CISD-2p and CIS-2p hereafter).

The single- and double-ionization cross sections are computed using the approach reported in detail in [8]. We only briefly summarize the methods and computational details here.

The total single-ionization (SI) cross sections $\sigma_{\rm SI}$ are computed as

$$\sigma_{\rm SI} = \sum_j^{N_{\rm IP}} \sigma_j + \sum_j^{N_{\rm DIP}} \left[2\times\mathcal{D}_j(1-\mathcal{D}_j)+\mathcal{D}_j^2\right]\sigma_j, \tag{5}$$

where $\mathcal{D}_j$ represents the probability that one electron in the pseudostate j is in a bound orbital of the cation. The latter are calculated using the Dyson model developed in [8]. Similarly, the total double-ionization cross sections $\sigma_{\rm DI}$ are computed as

$$\sigma_{\rm DI} = \sum_j^{N_{\rm DIP}} (1-\mathcal{D}_j)^2\sigma_j. \tag{6}$$

In the above equations, σ_j is the cross section of the pseudocontinuum state j. $N_{\rm IP}$ and $N_{\rm DIP}$ are, respectively, the number of pseudocontinuum states in the energy range between the ionization potential (IP) and double-ionization potential (DIP) and above the DIP. Note that we have added the contribution of the autoionization states to the $\sigma_{\rm SI}$.

Based on the Dyson model above, we compute the total electronic stopping cross section as

$$S_e^{\rm tot} = S_e^{\rm SE} + S_e^{\rm SI} + S_e^{\rm DI}, \tag{7}$$

where $S_e^{\rm SE}$, $S_e^{\rm SI}$, and $S_e^{\rm DI}$ are computed as

$$S_e^{\rm SE} = \sum_j^{N_{\rm SE}} (\epsilon_j - \epsilon_0)\sigma_j, \tag{8}$$

$$S_e^{\rm SI} = \sum_j^{N_{\rm IP}} (\epsilon_j - \epsilon_0)\sigma_j + \sum_j^{N_{\rm DIP}} \left[2\times\mathcal{D}_j(1-\mathcal{D}_j)+\mathcal{D}_j^2\right] \times (\epsilon_j - \epsilon_0)\sigma_j, \tag{9}$$

$$S_e^{\rm DI} = \sum_j^{N_{\rm DIP}} (1-\mathcal{D}_j)^2(\epsilon_j - \epsilon_0)\sigma_j. \tag{10}$$

In the above equations, SE stands for single excitation. $N_{\rm SE}$ is the number of pseudostates with energy lower than the ionization potential.

III. RESULTS AND DISCUSSION

A. Antiproton-neon collisions

We compare the present CISD results for total SI and DI cross sections with the experimental data of Paludan *et al*. [17] and Andersen *et al*. [18]. CIS results and other theoretical data of Lüdde *et al*. [2] (basis generator method, labeled BGM), Abdurakhmanov *et al*. [9] (semiclassical time-dependent convergent close-coupling approach, labeled CCC), and Montanari and Miraglia [19] (continuum distorted-wave eikonal initial-state approximation, labeled CDW-EIS, including postcollisional effects) are also shown in Fig. 1.

We first discuss the SI cross sections: our CISD results are close to the experimental data and the CCC cross sections. In contrast to the CISD and CCC results, our CIS calculations are comparable to the BGM ones (net and response). Both models predict larger SI cross sections than the other approaches. The BGM model includes electronic correlation only approximately in the framework of a DFT approach, CIS is an uncorrelated approach, while in the CISD model the correlation is better described by single and double excited configurations. That causes the differences and shows how important the electronic correlation is. Therefore, based on the comparison with CISD results we conclude that electronic correlation is crucial to obtain accurate cross sections. Note that the CCC calculations neglect completely the electronic correlation. The good agreement with CISD may be accidental or due to error cancellation. It should also be noted that in [9] (CCC) and in [19] (CDW-EIS) the authors use potentials for neon determined from Hartree-Fock wave functions. In the BGM calculations [2], the target potentials were described within the optimized potential method. In our paper, we use

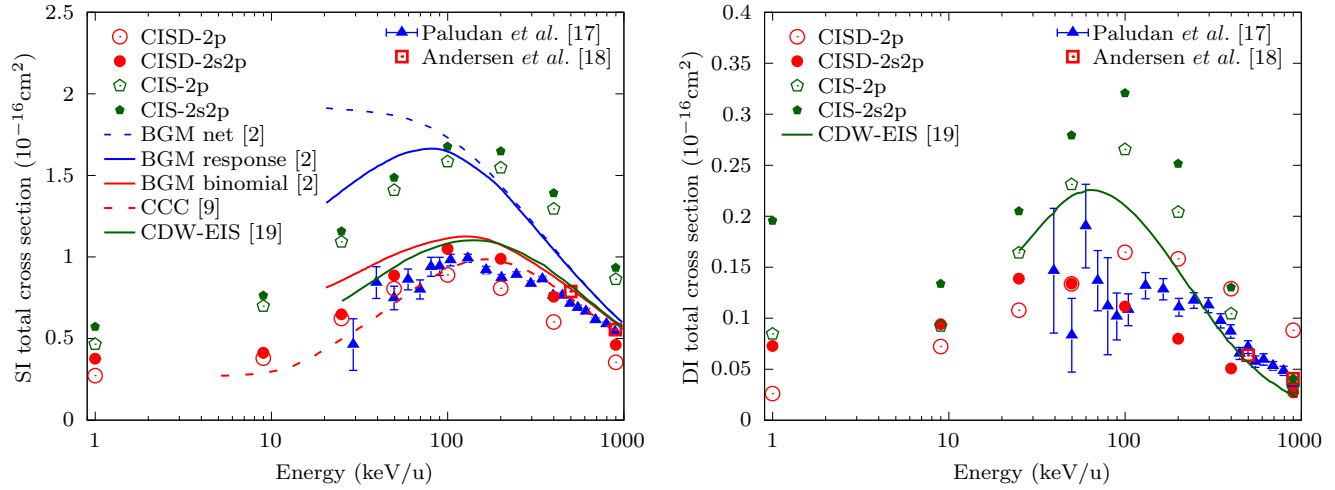

FIG. 1. Total cross sections for single ionization (left) and double ionization (right) of neon by antiproton impact plotted as functions of impact energy.

the true potentials. The use of different potentials might explain the observed differences.

The DI cross sections are shown in the right panel of Fig. 1. Our CISD results agree reasonably well with the experimental cross sections and the CDW-EIS calculations. Given the difficult task of describing multiple ionization processes the agreement between our results and previous data can be considered satisfactory. Conversely and similarly to the SI cross sections, the uncorrelated (CIS) approach overestimates the DI cross sections. It is also interesting to note that the CIS and CISD results accounting for the $2s$ electrons are larger in magnitude than those accounting only for the $2p$ electrons, except in the case of the CISD-$2p$ and CISD-$2s2p$ calculations at impact energies from 100 keV to 1 MeV. This suggests that the electronic correlation between the $2s$ and $2p$ electrons hinders the double ionization of neon at high collision energies. It should be noted that the difference between the CISD-$2p$ and CISD-$2s2p$ cross sections is much larger than the difference between the cross sections obtained with the two Gaussian basis sets. Therefore, despite the lower convergence of the DI cross sections, the impact of the electronic correlation is clearly observed.

We now turn our attention to the electronic stopping power. Figures 2 and 3 show the electronic stopping-power cross section computed by Eqs. (7)–(10) for the neon target case. Figure 2 is a Fano plot and we have included the Bethe cross sections [21] for comparison. The CISD results are compared to the BGM results of Lüdde *et al*. [2] and the CCC results (semiclassical time-dependent convergent close-coupling approach) of Bailey *et al*. [22]. Our correlated approach predicts cross sections much lower than the BGM one and closer to the CCC method. In [2], it was argued that the difference between the BGM and the CCC results could be due to the effects of the $2s$ electrons, that are kept frozen in the CCC calculations. However, the comparison between CISD-$2s2p$ and CISD-$2p$

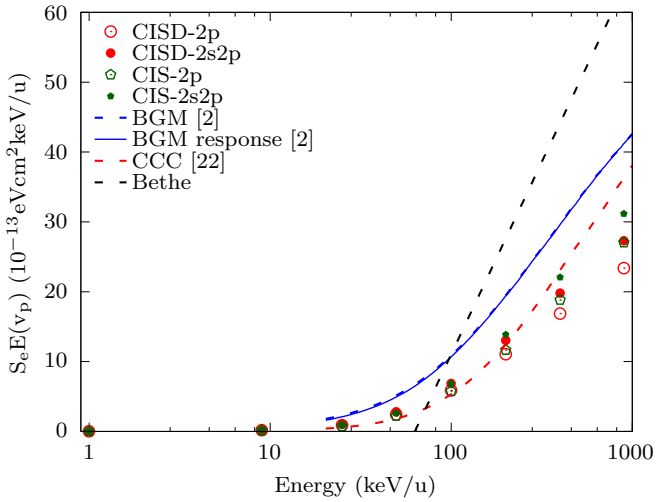

FIG. 2. Fano plot for antiproton-neon collisions. The stopping-power cross sections are computed with different models (see text). The Bethe cross sections were computed with a mean excitation energy of 137.2 eV [20].

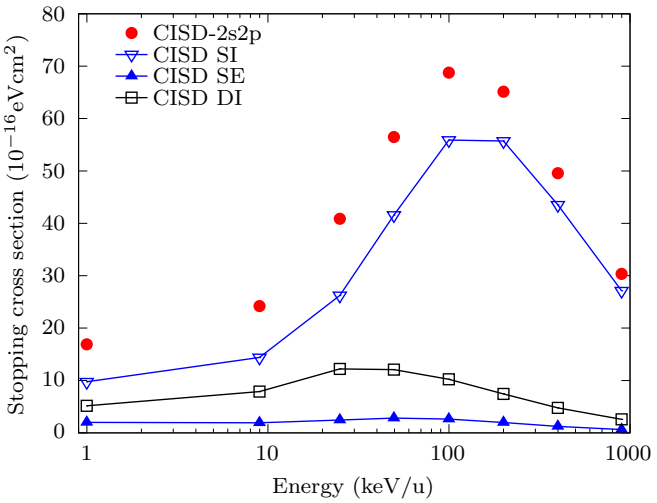

FIG. 3. Contribution of the different processes to the electronic stopping-power cross section as functions of impact energy.

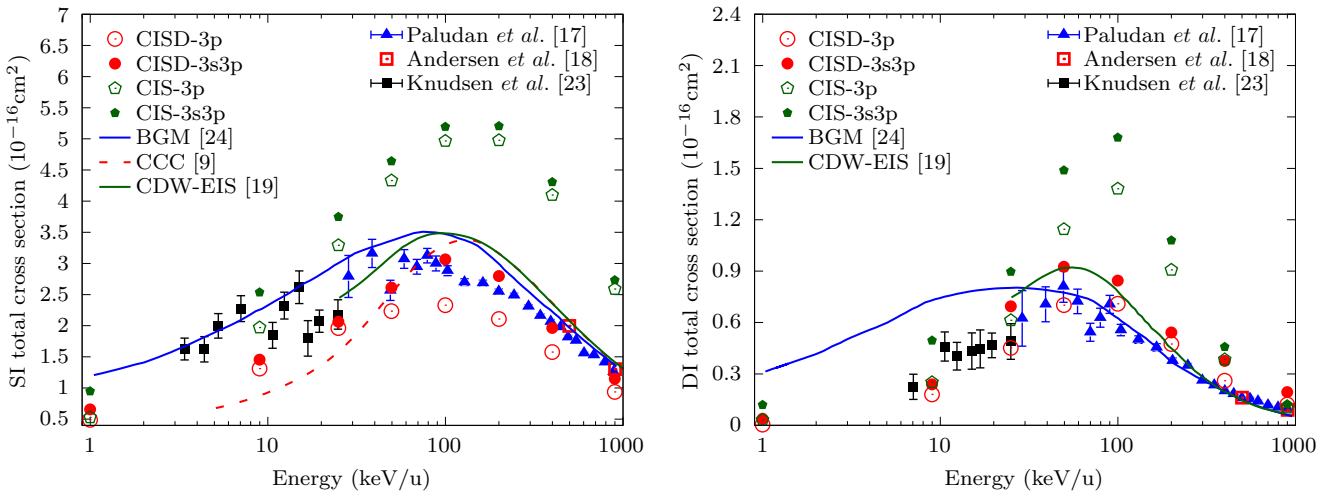

FIG. 4. Total cross sections for single ionization (left) and double ionization (right) of argon by antiproton impact plotted as functions of impact energy.

indicates that the contribution of 2*s* electrons cannot explain the difference.

In Fig. 3, we show the contribution of the different processes to the electronic stopping power. It is seen that the SI and DI contribute the most. Since the CCC calculations only consider SI their cross sections should be much lower. However, the lack of electronic correlation in the CCC model may overestimate the SI processes and therefore leads to error cancellation.

We conclude from these comparisons that the 2*s* electrons can be kept frozen but to obtain an accurate description of the stopping power the electronic correlation between the 2*p* electrons must be explicitly accounted for.

B. Antiproton-argon collisions

We also investigate the antiproton-argon collision system to determine if the conclusions drawn from the neon case are general. We compare the present CISD and CIS results (3*s* and 3*p* electrons, aug-cc-pVDZ-3kbj [14,15]) for total SI and DI ionization cross sections with the experimental data of Paludan *et al*. [17], Andersen *et al*. [18], and Knudsen *et al*. [23] and theoretical data of Kirchner *et al*. [24] (BGM), Abdurakhmanov *et al*. [9] (CCC), and Montanari and Miraglia [19] (CDW-EIS, including post collisional effects), as reported in Fig. 4. The electronic stopping power is shown in Figs. 5 (Fano plot) and 6 in which the CCC results are from Bailey *et al*. [22].

The SI cross sections from the CISD calculations are similar to those of the experiments. Similarly to the antiproton-neon collisions, the CIS cross sections are much larger than the CISD results, illustrating again the importance of the electronic correlation.

The electronic stopping-power cross sections computed with the different models are reported in Fig. 5. The four models predict the same cross sections within 20%. Compared

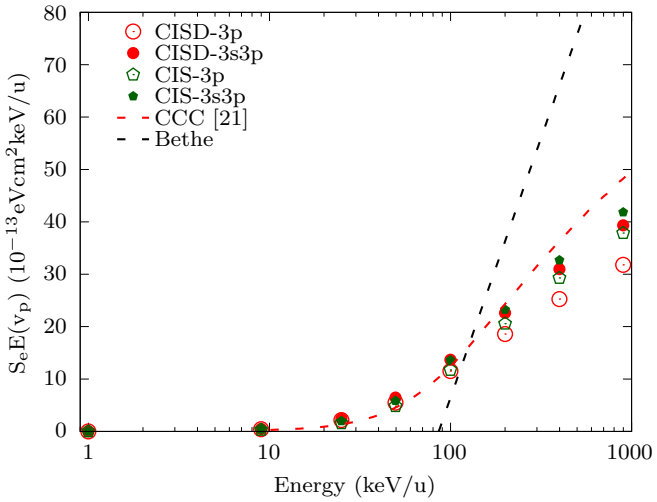

FIG. 5. Fano plot for antiproton-argon collisions. The stopping-power cross sections are computed with different models (see text). The Bethe cross sections were computed with a mean excitation energy of 188.5 eV [20].

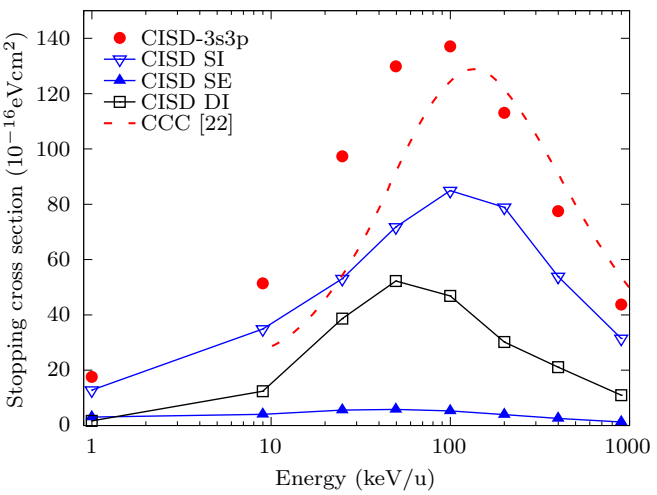

FIG. 6. Contribution of the different processes to the electronic stopping-power cross section as functions of impact energy.

to the CCC results, the cross sections exhibit a similar bell shape but our cross sections peak at slightly lower energy.

The contributions of the different processes to the electronic stopping-power cross sections are shown in Fig. 6. Similarly to the neon case, SI contributes the most. However, the DI contribution is relatively larger for argon than for neon for collision energies above 10 keV/u.

IV. CONCLUSIONS

In conclusion, we studied collisions between antiprotons and the rare-gas atoms neon and argon in the keV energy range. Our theoretical approach employs a correlated approach in which the eight electrons from the L shell of neon and M shell of argon are active and up to two-electron processes are explicitly taken into account. We showed that the electronic correlation plays a major role for an accurate description of single- and double-ionization processes. Furthermore, our results demonstrated that two-electron processes contribute significantly to the electronic stopping power. These results apply to neon and argon target atoms and we therefore conclude that a correlated approach is in general necessary to investigate antiproton collisions. Our paper paves the way to a more accurate description, and thus understanding, of antiproton physics.

ACKNOWLEDGMENTS

C.C.J. is supported by a China Scholarship Council (CSC) scholarship within a CSC-SU program. J.W.G., Y.W. and J.G.W. acknowledge the supports of the National Natural Science Foundation of China (Grants No. 11934004 and No. 12374229).

[1] S. Borbély, X.-M. Tong, S. Nagele, J. Feist, I. Březinová, F. Lackner, L. Nagy, K. Tőkési, and J. Burgdörfer, Phys. Rev. A **98**, 012707 (2018).
[2] H. J. Lüdde, M. Horbatsch, and T. Kirchner, Phys. Rev. A **104**, 032813 (2021).
[3] K. Nordlund, M. Hori, and D. Sundholm, Phys. Rev. A **106**, 012803 (2022).
[4] See https://espace.cern.ch/elena-project/SitePages/Home.aspx.
[5] See https://home.cern/news/news/accelerators/ls2-report-waiting-antiprotons.
[6] M. Schulz, *Ion-Atom Collisions: The Few-Body Problem in Dynamic Systems* (de Gruyter, Berlin, Germany, 2019).
[7] T. Kirchner and H. Knudsen, J. Phys. B **44**, 122001 (2011).
[8] C. C. Jia, T. Kirchner, J. W. Gao, Y. Wu, J. G. Wang, and N. Sisourat, Phys. Rev. A **107**, 012808 (2023).
[9] I. B. Abdurakhmanov, A. S. Kadyrov, D. V. Fursa, S. K. Avazbaev, J. J. Bailey, and I. Bray, Phys. Rev. A **91**, 022712 (2015).
[10] N. Sisourat, I. Pilskog, and A. Dubois, Phys. Rev. A **84**, 052722 (2011).
[11] J. W. Gao, Y. Wu, N. Sisourat, J. G. Wang, and A. Dubois, Phys. Rev. A **96**, 052703 (2017).
[12] J. W. Gao, Y. Wu, J. G. Wang, N. Sisourat, and A. Dubois, Phys. Rev. A **97**, 052709 (2018).
[13] J. W. Gao, Y. Wu, J. G. Wang, A. Dubois, and N. Sisourat, Phys. Rev. Lett. **122**, 093402 (2019).
[14] B. P. Pritchard, D. Altarawy, B. Didier, T. D. Gibson, and T. L. Windus, J. Chem. Inf. Model. **59**, 4814 (2019).
[15] K. Kaufmann, W. Baumeister, and M. Jungen, J. Phys. B **22**, 2223 (1989).
[16] See Supplemental Material at http://link.aps.org/supplemental/10.1103/PhysRevA.110.012803 for details of the basis sets.
[17] K. Paludan, H. Bluhme, H. Knudsen, U. Mikkelsen, S. Møller, E. Uggerhøj, and E. Morenzoni, J. Phys. B **30**, 3951 (1997).
[18] L. H. Andersen, P. Hvelplund, H. Knudsen, S. P. Moller, A. H. Sorensen, K. Elsener, K.-G. Rensfelt, and E. Uggerhoj, Phys. Rev. A **36**, 3612 (1987).
[19] C. C. Montanari and J. E. Miraglia, J. Phys. B **45**, 105201 (2012).
[20] S. P. Sauer, J. Oddershede, and J. R. Sabin, in *Concepts of Mathematical Physics in Chemistry: A Tribute to Frank E. Harris—Part A*, Advances in Quantum Chemistry Vol. 71, edited by J. R. Sabin and R. Cabrera-Trujillo (Academic, New York, 2015), pp. 29–40.
[21] H. Bethe, Ann. Phys. (NY) **397**, 325 (1930).
[22] J. J. Bailey, A. S. Kadyrov, I. B. Abdurakhmanov, D. V. Fursa, and I. Bray, Phys. Rev. A **92**, 022707 (2015).
[23] H. Knudsen, H.-P. E. Kristiansen, H. D. Thomsen, U. I. Uggerhøj, T. Ichioka, S. P. Møller, C. A. Hunniford, R. W. McCullough, M. Charlton, N. Kuroda, Y. Nagata, H. A. Torii, Y. Yamazaki, H. Imao, H. H. Andersen, and K. Tökesi, Phys. Rev. Lett. **101**, 043201 (2008).
[24] T. Kirchner, M. Horbatsch, and H. J. Lüdde, Phys. Rev. A **66**, 052719 (2002).